ELECTROCATALYSIS IN THE NICKEL-TITANIUM SYSTEM

Eduard W. Justi, Henning H. Ewe, Adolf W. Kalberlah, Nikolaus M. Saridakis, and Martin H. Schaefer

Institute of Technical Physics, University of Braunschweig
Braunschweig, West Germany

1. INTRODUCTION

Europe offers no economic chances for application of fuel cells in military or space technology and therefore, all efforts are focussed to eventual applications in civilian technique. This has been the reason why Justi, Scheibe, and Winsel (1) have postulated from their beginnings in the early fifties to avoid principally rare metal electrocatalysts when publishing their double skeleton katalyst ("DSK") system of fuel cells. To achieve the necessary high catalytic activity of base metal catalysts operating at ambient temperature they have introduced into electrochemistry for the first time Raney type microskeleton catalysts supported by inactive macroskeleton electrodes. Raney nickel in hydrogen anodes, and Raney silver oxygen (air) cathodes or similar structures are now widely used even in other countries for fuel cells operating with alkaline electrolytes at ambient temperature and low pressure. In the meantime Justi et al. (2) have investigated various other base metals concerning their abililty as electrocatalysts and focussed their present interest to titanium which appears attractive for its low specific weight and huge hydrogen storage capacity, up to the nonstoichiometric hydride $TiH_{1.65}$.

Unfortunately titanium is corroding in alkaline electrolytes by formation of irreducible impermeable TiO_2 (rutile) coating layers thus excluding application in our fuel cell system. Moreover the above mentioned huge hydrogen storage capacity cannot be used efficiently by adsorbing hydrogen at moderate temperatures and subsequent desorption at high temperatures. For by this method of storing hydrogen about one half of the free energy of combustion of hydrogen would be wasted, as we have calculated by applying a Carnot cycle on experimental data such as temperatures, pressures, heat content, and heats of sorption. Therefore the goal of the present work is to combine the good catalytic and storing properties of nickel and titanium, and to avoid the disadvantageous ones, both for fuel cell and for accumulator electrodes. Of course this cannot be done simply by mixing both metals and thus averaging their various properties. However nickel and titanium are forming some intermetallic compounds stable by relatively high energies of formation (about 8000 cal/mole) with quite differing properties. These compounds and their

alloys may offer a chance of finding out electrocatalysts with really new and possibly favourable performance. To find this assertion plausible look at the complicated structure of the elementary cell of Ti_2Ni crystal containing 96 atoms (fig. 1) and offering at least 3 different distances between Ti-Ti, Ni-Ni, and Ni-Ti atoms, an increased tendency towards covalency between Ti and Ni atoms, and a corresponding variety of hydrogen binding energies (3).

2. DIAGRAM OF STATE OF THE BINARY SYSTEM Ti-Ni AND SCOPE OF PRESENT WORK

According to the well known diagram of state (4) Ti and Ni form the intermetallic compounds Ti_2Ni, TiNi, and $TiNi_3$, out of which we have investigated Ti_2Ni and TiNi. As the left side of fig. 2 shows, Ti_2Ni forms an eutecticum with ß-Ti. Therefore, all alloys containing less than 33.3 at-% Ni have finely dispersed Ti corroding in lyes and forming the above mentioned thick layer of irreducible TiO_2. This is the reason why we have focussed our efforts to the interval between Ti_2Ni and TiNi, this is from 33.3 to 50 at-% Ni. The diagram of state shows that cooling down a melt of e. g. 43 at-% Ni starts with precipitation of TiNi thus enriching the residual melt with Ti. Continued cooling causes increased segregation of TiNi, until at 1015°C Ti_2Ni is formed by peritectic reaction of TiNi and the residual melt. A typical example of such a peritectic structure is shown in the micrograph fig. 3 at 250 times linear magnification. The rounded off parts of the structure are the residuals of primarily precipitated TiNi grains surrounded by peritecticly formed Ti_2Ni.

For our experiments we have chosen several alloys with different contents of Ti_2Ni and TiNi. Concerning the TiNi-rich alloys a difficulty arises because TiNi is extremely hard and tough and can neither be rolled nor powdered. The nickel richest composition we were able to mill contained 53.6 at-% Ti and 46.4 at-% Ni. In this case the TiNi grains are prevailing but are surrounded completely by the brittle Ti_2Ni-regions, a circumstance of importance for our results to be reported.

3. STORAGE OF CATHODICALLY EVOLVED HYDROGEN

First of all we would like to learn if and how this alloy will accept cathodically evolved hydrogen. For this purpose we have pressed and sintered DSK electrodes consisting of 3 gramms of the particular Ti_2Ni-TiNi alloy with grain sizes from 35 to 150 microns, and 6 gramms copper with grain sizes below 6 microns as a soft macroskeleton preventing formation of cracks caused by volume increase of hydrogen accepting titanium. This circular electrodes of 40 mm diameter, corresponding to twice 12 sq. cm geometric surface were charged first with 5 mA cathodically in 6m KOH at ambient temperature. Fig. 4 shows the potentials of several specimens thus measured vs. reversible hydrogen potential as function of the charge accepted. The potentials start rather negative

and subsequently become somewhat more positive. This transient positive sign of potential may be explained by supposing an autocatalytic mechanism (5), this means the primarily accepted hydrogen will favour subsequent entering of H-atoms. Probably this effect is caused by enlargement of the crystal lattice facilitating the inclusion of additional hydrogen until complete saturation.

Next diagram fig. 5 shows the slow anodic discharge of same electrodes at same current strength. There are striking differences between charging and discharging capacities. This difference may be called "irreversible capacity" or "first hydrogen" and is plotted in fig. 6 vs. Ni content of each specimen and one may conclude that only Ti_2Ni will bind the hydrogen so strongly. In this connection let us remember the complicated structure of the Ti_2Ni crystal cell (fig. 1) offering a variety of interatomic distances and thus binding energies. More precise measurements, taking into account an initial corrosion of Ti_2Ni have shown that one molecule of Ti_2Ni may trap irreversibly about two hydrogen atoms. However, concerning the storage capacity of the system Ti-Ni mainly hydrogen dischargeable in the region of reversible hydrogen potential - this is up to 200 mv against reversible hydrogen - is of practical importance. These reversible capacities are plotted vs. Ni-content of each alloy in fig. 7, and one may see that they decrease with Ni-content linearly, so the useful capacity is composed additively of those of the pure compounds Ti_2Ni and TiNi. Only the values of the Ti_2Ni richest compositions are deviating from this linearity. Micrographs have shown that these deviations may be caused by insufficient breaking of alloys containing only a few grain boundaries. Therefore, we have feeled justified to calculate the specific capacities of the pure compounds Ti_2Ni and TiNi by linear extrapolation of these measuring values of the alloys. Thus the specific useful capacity of pure Ti_2Ni amounts to 0.26 , and that of pure TiNi to 0.245 amp. hrs/gramm. This means, that each molecule of Ti_2Ni may store about 1.5 , and each molecule of TiNi about 1 H-atom in a reversible way, and this hydrogen may be called "second hydrogen".

According to our hope mentioned in our introduction the reversible specific capacity is rather high, but there are several other important points of view for the evaluation of an accumulator electrode, such as fast charge acceptance, high discharging rate, aging properties and so on. Ti_2Ni offers excellent fast discharge performance, for the capacity decreases but little on discharge rates down to 15 minutes ("4 C"). In contrast to Ti_2Ni, the capacity of TiNi decreases with increasing discharge rate, what may be explained by slower diffusion of H-atoms within the TiNi crystal lattice.

To evaluate the cycling performance we have checked the above mentioned specimens by automatic cycling at a six hours rate (C/6) within a potential interval from -30 to + 200 mv vs. reversible hydrogen electrode in the same electrolyte 6m KOH at room temperature. The discharge capacity of Ti_2Ni rich electrodes degraded to 50% after 45 cycles already, whereas TiNi rich specimens, e. g. 53.6 at-% Ti and

46.4 at-% Ni reached this deterioration but after 300 cycles.

One may conclude that it is mainly Ti_2Ni which is responsible for aging of the alloys. This result could be confirmed directly by microscopic inspection of polished and etched specimens containing 57 at-% Ti and 43 at-% Ni, and comparing a virgin sample with another after 180 cycles. Fig. 8 demonstrates that TiNi grains remain unaffected, whereas the surrounding Ti_2Ni regions became completely black under cycling. The information given by light microscopy have encouraged us to apply larger magnifications using an electron microscope and in addition to elucidate the structure and composition by electron beam probe. Fig. 9a corroborates at 1000x linear magnification that TiNi grains remain unchanged. Fig. 9b shows a monochromatic photo of the nickel X-ray radiation and indicates that the surface of TiNi grains is enriched in nickel. In contrast, the original Ti_2Ni phase has lost most of its nickel. Fig. 9c is a monochromatic picture of Ti radiation and shows that Ti atoms are distributed rather homogeneously. Fig. 9d proves an enrichement of potassium atoms in the areas of former Ti_2Ni grains. Another analysis has disclosed an enrichement of about 20% oxygen there, and both K and O atoms must have entered from electrolyte.

However, the decrease of useful capacity of TiNi rich alloys under cycling cannot be explained by Ti_2Ni oxidation only, for the capacity of TiNi grains should remain unaltered. According to fig. 8 the TiNi grains are surrounded by peritecticly formed Ti_2Ni respectively the impermeable coating layers formed by its oxidation, preventing the access of hydrogen.

4. HYDROGEN ADSORPTION FROM GASEOUS PHASE

After the adsorption of cathodically evolved hydrogen by various Ti-Ni compounds we have studied the corresponding acceptance from gaseous molecular hydrogen. For this purpose we used electrodes with the data mentioned above. These electrodes were now provided with an additional fine pore copper coating layer, and after being fitted in a conventional gas tight half cell arrangement with 6m KOH as electrolyte, hydrogen was admitted at pressure of 2 atmospheres to the active side of the electrode. In fig. 10 is plotted the hydrogen consumption Q(t) measured in amp. hrs equivalents per gramm alloy containing 64 at-% Ti and 36 at-% Ni, vs. time t in hours. The saturation value is about 0.44 amp. hrs/gramm, this is as much as from cathodically evolved hydrogen (cf. fig. 4). The adsorption velocity $\dot{Q}(t)$ of hydrogen is obtained by differentiating Q(t), and is also plotted in fig. 10 vs. time. As one may see, the adsorption starts very slowly following an exponential function and reaching its maximum after 7.5 hours. This dependence on time may be explained by an autocatalytic mechanism similar to the course of potential during the first cathodic charging as described above, cf. fig. 4.

By this arrangement we have checked all our alloys and confirmed that they are able to adsorb molecular hydrogen from the gaseous phase. Hydrogen adsorbed in this way may also be discharged electrochemically and therefore, this alloy is suitable as electrocatalyst in H_2 anodes.

5. HYDROGEN ANODES

However, for application of said Ti-Ni compounds and alloys as catalysts in hydrogen anodes, adsorption of molecular hydrogen does not suffice; in addition is deciding the voltage amperage performance. For this purpose we have made circular gas diffusion electrodes of 40 mm diameter consisting of an active layer containing 3 gramm Ti-Ni compounds alloy with grain size below 60 microns, 6 gramm electrolytic copper as macroskeleton and 1.5 gramm Na_2CO_3 with grain size below 75 microns as filler. This active layer was coated by 2 gramm of copper as fine pore coating layer and hot pressed at 400 °C under 8 tons. Among the various compositions of active materials, the Ti_2Ni rich mixtures were hydrogenated before hot pressing to prevent subsequent formation of cracks under hydrogen adsorption.

These electrode specimens were operated both as cathodes or anodes in an hydrogen atmosphere of 2 atm at room temperature. Fig. 11 shows the current polarization performance for both directions of processing and a slope of 3.5 to 6 ohm. cm^2, and this differential resistance compares unfavourably with good Raney nickel DSK electrodes reaching values below 1.5 ohm. cm^2. To specify the reason for this insufficient performance we have first measured the current density as function of temperature and plotted in an Arrhenius diagram delivering a linear correlation between logarithm of amperage and inverse operating temperature with a slope corresponding to 4 to 5.5 kcal/mole, rather independent on Ti_2Ni to TiNi ratio and equalling those of good Raney nickel. Therefore, the inner surface became suspicious to be insufficient. In fact, BET measurements have disclosed that the inner surface of TiNi rich alloys is less than 1 sq. m/gramm, this is only 1 percent of our Raney nickel.

6. OUTLOOK

Although our investigations into the electrocatalytic properties of alloys of intermetallic Ti-Ni compounds have not yet yielded a technical progress we are finding it encouraging that intermetallic compounds are offering a new variety of potential electrocatalysts, in addition to the hitherto applied metallic elements. Moreover the electron beam probe has proved to be a very useful tool in analyzing electrode structures and in fact we have quite recently succeeded in increasing the inner surface of the tough compound TiNi and reached the cathodic and anodic performances shown in the last diagram (fig. 12) equalling the values of good Raney nickel. So one may hope to make a breakthrough in this way.

ACKNOWLEDGMENTS

We should like to express our gratitude to Professor O. Rüdiger, director of the Krupp Central Research Institute, Essen, for preparing

the alloys and for stimulating discussions. The authors wish also to thank their sponsors, Siemens AG in Erlangen, and Varta AG in Frankfurt, West Germany, for their support and permission to publish this work.

REFERENCES

(1) Justi, E., Scheibe, W., and Winsel, A.: DBP 1 019 361 (1954); Brit. Pat. 806 644; US Pat. 2 928 891 (1954).

(2) Justi, E. W., and Winsel, A. W., "Cold Combustion - Fuel Cells", Fr. Steiner Publ., Wiesbaden, Germany, (1962); J. Electrochem. Soc. 108, 1073 (1961).

(3) Yurko, G. A., Barton, J. W., and Parr, J. Gordon, Acta Cryst. 12, 909 (1959).
Kubaschewski, O., Trans. Faraday Soc. 54, 814 (1958).
Hume-Rothery, W., and Coles, B. R., Advances in Physics 3, 149 (1954).
Pauling, L., J. Amer. Chem. Soc. 69, 542 (1947).

(4) Hansen, M., "Constitution of Binary Alloys", McGraw-Hill Book Co., New York, (1958).

(5) Kalberlah, A. W., and Winsel, A. W., Z. Elektrochem., Ber. Bunsenges. physik. Chem. 68, 250 (1964).

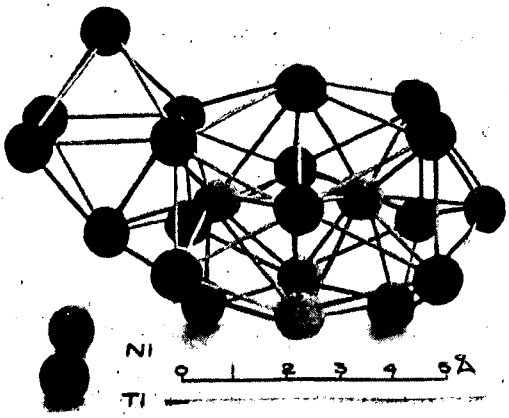

Fig. 1. Representative portion of Ti_2Ni cell.

Fig. 3. Photomicrograph of Ti-Ni alloy with 43 atomic per cent nickel. Etched in a mixture of 2 cm^3 HF, 2 cm^3 HNO_3 and 96 cm^3 water.

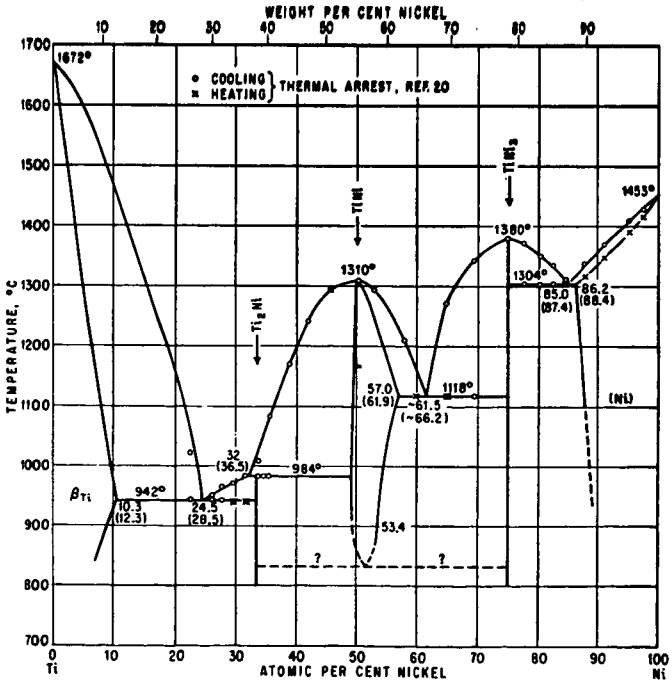

Fig. 2. Titanium-nickel phase diagram

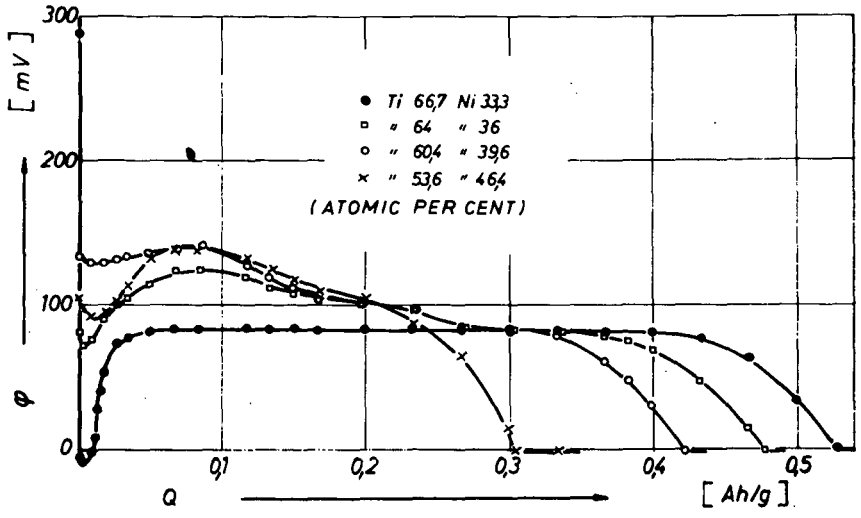

Fig. 4. Potential φ vs. hydrogen electrode in the same electrolyte of four electrodes with various Ti-Ni alloys as function of electric charge Q (in amp. hours per gramm Ti-Ni alloy) during the first galvanostatic kathodic charging process with 5 mA.

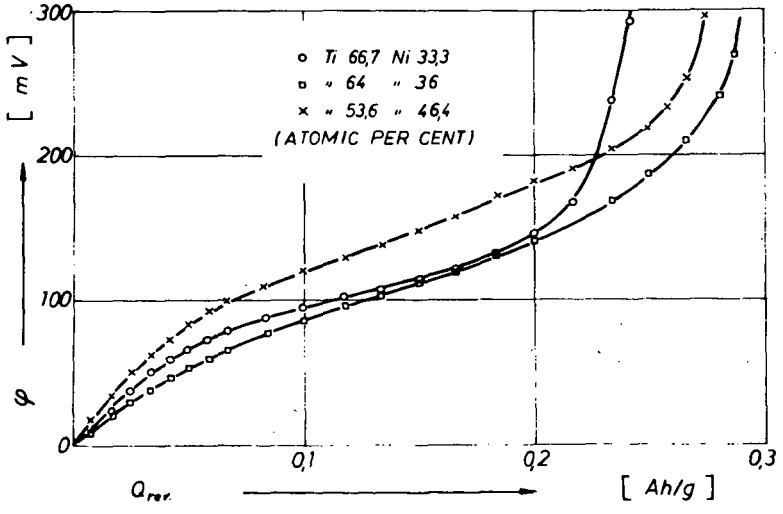

Fig. 5. Potential-charge plots of three electrodes during first anodic discharge with 5 mA following the cathodic charge of Fig. 4.

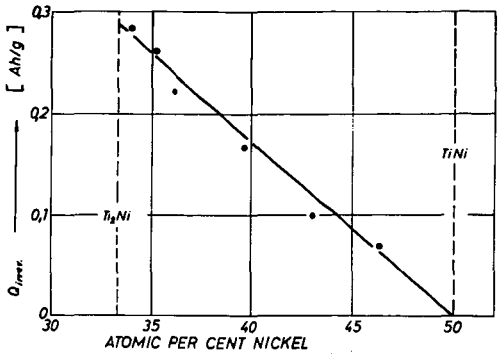

Fig. 6. Irreversible hydrogen storage capacity $Q_{irrev.}$ of one gramm Ti-Ni alloy vs. its composition.

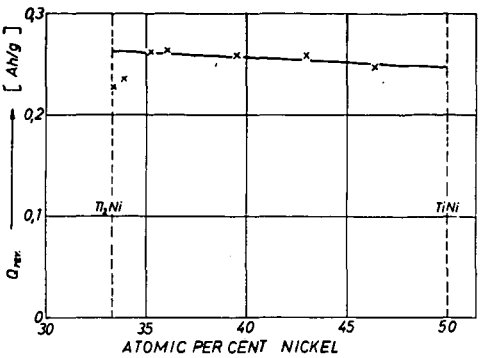

Fig. 7. Reversible hydrogen storage capacity $Q_{rev.}$ of one gramm Ti-Ni alloy vs. its composition.

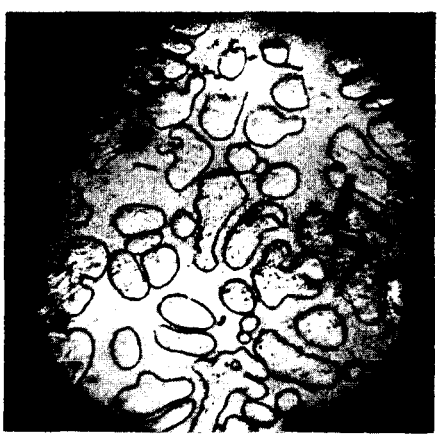

Fig. 8a.

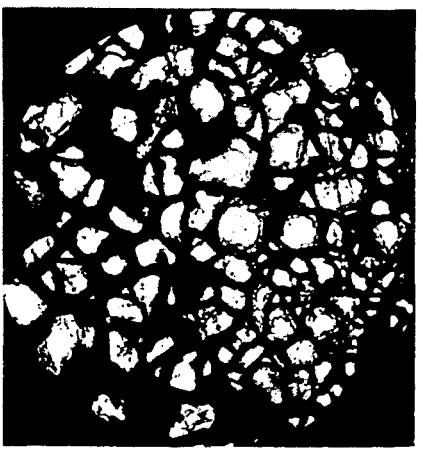

Fig. 8b.

Photomicrographs of Ti-Ni alloy grains (43 atomic per cent nickel), showing TiNi surrounded by Ti_2Ni

a) before any electrochemical treatment

b) after 180 charge discharge cycles, etching, cf. Fig. 3.

Fig. 9. Electron microprobe analysis of a Ti-Ni alloy grain (43 atomic per cent nickel), after 180 charge discharge cycles.

Fig. 9a. Electron image

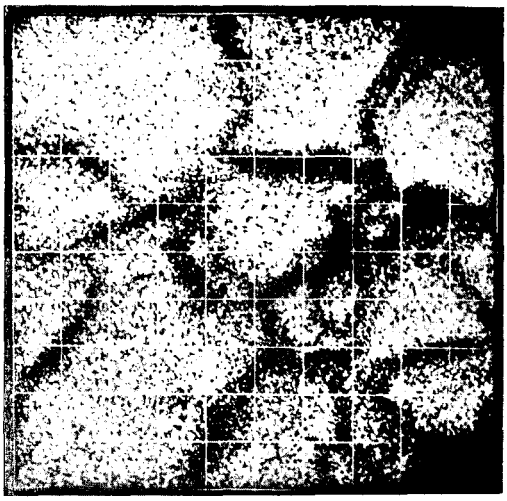

Fig. 9b. Distribution of Ni

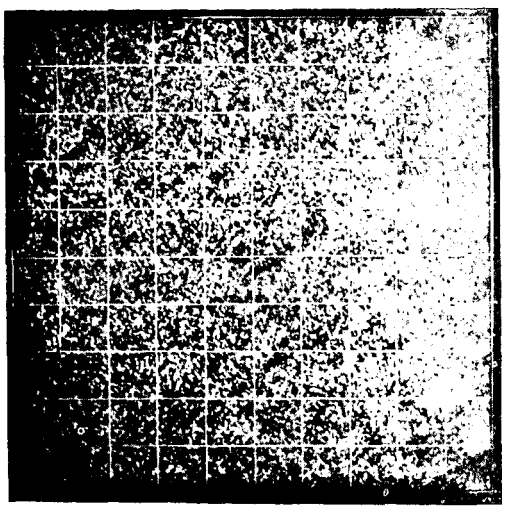

Fig. 9c. Distribution of Ti

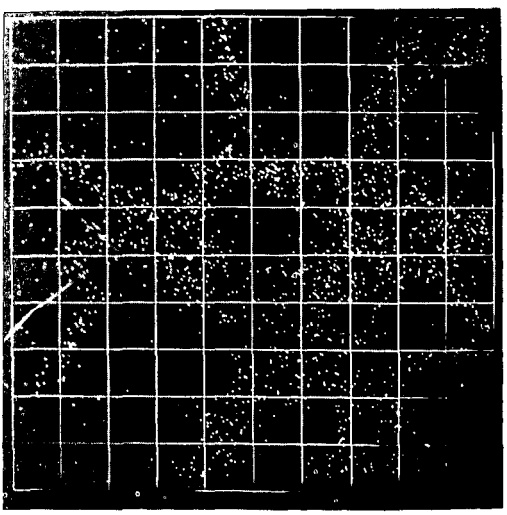

Fig. 9d. Distribution of K

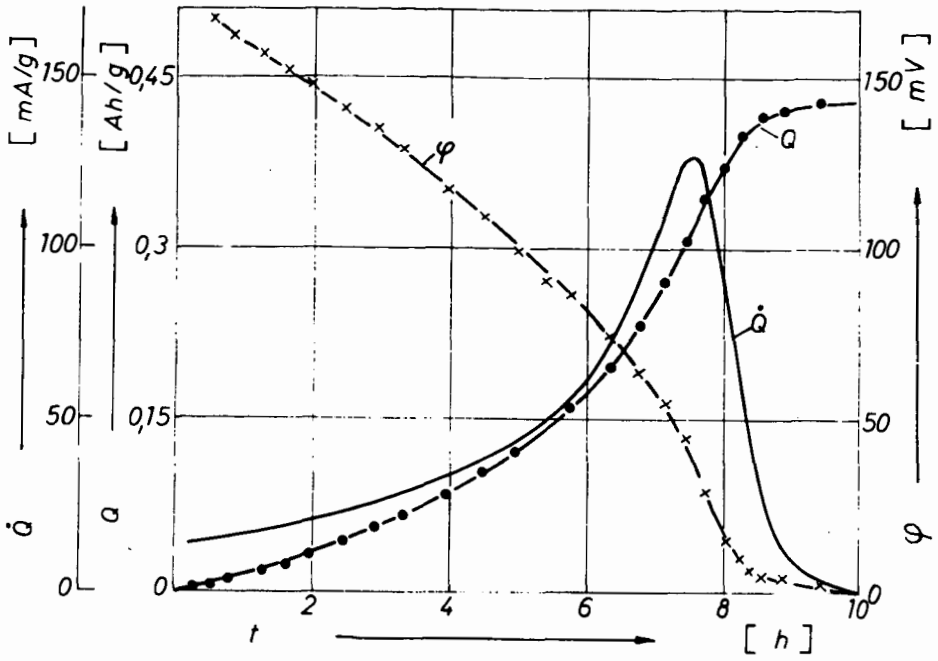

Fig. 10. First acceptance of hydrogen from the gasphase by an electrode with Ti-Ni alloy. Electrode potential φ against hydrogen electrode in the same electrolyte, accepted amount Q of hydrogen (expressed in Ah per gramm alloy) and influx $\dot{Q}$ of hydrogen in mA per gramm vs. time t in hours, 22°C.

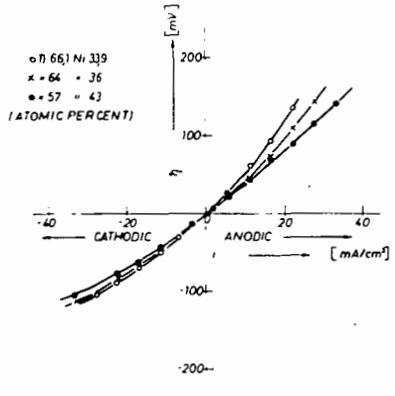

Fig. 11. Polarization-current density plots of three hydrogen electrodes with different Ti-Ni alloys as catalyst.

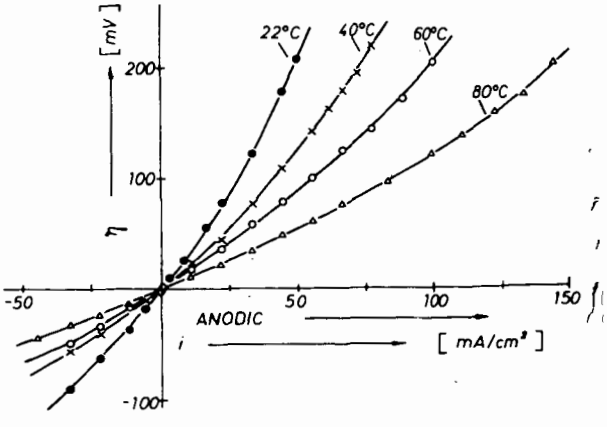

Fig. 12. Polarization-current density plots of a hydrogen electrode with TiNi as catalyst at different temperatures. Hydrogen pressure: 2 atmospheres.